Gyrokinetic particle simulations of toroidal momentum transport

I. Holod[a] and Z. Lin
Department of Physics and Astronomy, University of California, Irvine, California 92697, USA

(Received 10 June 2008; accepted 11 August 2008; published online 10 September 2008)

Simulations of toroidal angular momentum transport have been carried out using global toroidal gyrokinetic particle-in-cell code. The significant redistribution of toroidal momentum is observed, driven by the ion temperature gradient turbulence with adiabatic electrons, resulting in a peaked momentum profile in the central region of the radial domain. Cases with rigid and sheared plasma rotation are considered. Diffusive and off-diagonal (pinchlike) fluxes are identified. Toroidal momentum diffusivity is calculated by subtracting pinch contribution from the total momentum flux, and compared to quasilinear estimates. It is found that the ratio of momentum to heat conductivity is smaller than unity even after subtracting pinch contribution when wave-particle resonance energy is larger than thermal energy. © *2008 American Institute of Physics*. [DOI: 10.1063/1.2977769]

I. INTRODUCTION

Plasma rotation plays important role in turbulence stabilization[1,2] and in suppression of resistive wall modes,[3] therefore affecting tokamak performance. In present day machines, rotation is usually driven by external sources, such as neutral beam injection; however, it might be unavailable in a future devices such as ITER, due to the large machine size and high densities. Possible solution of this problem could be generation of spontaneous (intrinsic) rotation and on-axis peaking of momentum profile by inward pinchlike flux. Thus, it becomes crucial to understand the nature of intrinsic rotation phenomena, together with momentum transport mechanisms.

Substantial spontaneous rotation has been observed on many devices, such as JET,[4] Alcator C-Mod,[5] Tore Supra,[6] DIII-D,[7] TCV,[8,9] and JT-60U.[10] These and other experimental results are summarized and discussed in Ref. 11. Another important observation is the requirement of inward radial flow (pinch) of toroidal momentum in order to explain the experimental profile structure.[12] Toroidal momentum transport has been characterized by the momentum conductivity χ_ϕ. The ratio of χ_ϕ to the ion heat conductivity χ_i, called the Prandtl number ($\mathrm{Pr}=\chi_\phi/\chi_i$), has been theoretically predicted to be close to unity.[13,14] This conclusion is consistent with the fact that momentum confinement time is often comparable to the energy confinement time,[15,16] however, recent experiments report smaller values of Pr.[17,18]

There are several theoretical works attempting to describe the complicated nature of momentum transport.[19–26] The existence of nondiffusive (off-diagonal) contribution to the momentum flux is anticipated as the result of toroidal symmetry breaking. Simplified description, using quasilinear theory and mixing length estimates, is applied to describe momentum transport in fluid models.[27,28] The Prandtl number is found to be between 0.1 and 1, which is in approximate agreement with experiment, while off-diagonal contribution is not always treated correctly.

There have been recent works on gyrokinetic simulations of toroidal momentum transport driven by ion temperature gradient (ITG) mode.[14,29] In linear simulations by Peeters and Angioni[14] the Prandtl number is found to be close to 1 and weakly dependent on plasma parameters. In the nonlinear flux tube simulations using GYRO code,[29] the ratio of momentum to heat conductivity $\mathrm{Pr}\sim 0.8$ has been reported and an off-diagonal part of momentum transport has been observed.

In this paper we present the global nonlinear gyrokinetic simulations using gyrokinetic toroidal code (GTC).[30] Toroidal momentum transport is driven by ITG turbulence assuming no poloidal rotation. As the result of simulation we obtain flux surface averaged radial profiles of toroidal momentum and momentum flux, as well as time evolution of these quantities. Diffusive and pinch fluxes are identified for the wide range of simulation parameters. Prandtl number is found between 0.2 and 0.7, compared to a quasilinear estimate of $\mathrm{Pr}\sim 0.7$ based on obtained fluctuation spectra. This is in agreement with general conclusion that the Prandtl number is smaller than unity when the wave-particle resonance energy is larger than the thermal energy.

II. MODEL DESCRIPTION

In GTC, particle equations of motion are solved together with nonlinear gyrokinetic equation for the perturbed distribution function. For simulations of ITG turbulence electrostatic description is used, assuming Boltzmann distribution for electrons. The ions are treated kinetically.

The equilibrium ion distribution function F_0 is chosen to be the local Maxwellian shifted in parallel velocity,

$$F_{LM}(\varepsilon,\mu,\psi)=\frac{n(\psi)}{(2\pi T(\psi)/m)^{3/2}}\times\exp\left[-\frac{2\mu B-m(v_\parallel-u(\psi))^2}{2T(\psi)}\right], \quad (1)$$

where

[a]Electronic mail: iholod@uci.edu.

$$v_\parallel = \sigma\sqrt{\frac{2}{m}(\varepsilon - \mu B - e\Phi)}$$

is the velocity parallel to the equilibrium magnetic field $\mathbf{B}=B\hat{\mathbf{b}}$, $\sigma=\pm 1$ is the velocity sign, ε is the particle energy, Φ is the equilibrium electrostatic potential, and ψ is the poloidal magnetic flux.

For a high aspect ratio tokamak, assuming large and purely toroidal rotation (neglecting diamagnetic flow), the radial force balance takes a form

$$-\nabla\Phi + \frac{1}{c}u\hat{\mathbf{e}}_\phi \times \mathbf{B} = 0. \tag{2}$$

Writing a general axisymmetric magnetic field as

$$\mathbf{B} = I\nabla\phi + \nabla\phi\times\nabla\psi$$

and substituting $u=R\omega_\phi$, we obtain from Eq. (2),

$$c\Phi'(\psi) = -\omega_\phi(\psi). \tag{3}$$

Representing the ion distribution function as the sum of equilibrium F_0 and perturbed part δf, the gyrokinetic equation can be written as

$$\frac{1}{F_0}\left[\frac{\partial}{\partial t} + (v_\parallel\hat{\mathbf{b}} + \mathbf{v}_E + \mathbf{v}_d)\cdot\nabla - e(v_\parallel\hat{\mathbf{b}} + \mathbf{v}_E + \mathbf{v}_d)\cdot\nabla\delta\phi\frac{\partial}{\partial\varepsilon}\right]\delta f = -\tilde{\mathbf{v}}_E\cdot\frac{\nabla F_0}{F_0} + e(v_\parallel\hat{\mathbf{b}} + \bar{\mathbf{v}}_E + \mathbf{v}_d)\cdot\nabla\delta\phi\frac{1}{F_0}\frac{\partial F_0}{\partial\varepsilon}, \tag{4}$$

where $E\times B$ drift velocity $\mathbf{v}_E=\bar{\mathbf{v}}_E+\tilde{\mathbf{v}}_E$, $\bar{\mathbf{v}}_E=c/B\hat{\mathbf{b}}\times\nabla\Phi$, $\tilde{\mathbf{v}}_E=c/B\hat{\mathbf{b}}\times\nabla\delta\phi$, and magnetic drift velocity $\mathbf{v}_d=(\mu B/m+v_\parallel^2)\hat{\mathbf{b}}\times\nabla B/\Omega B$.

Taking into account the form of equilibrium distribution function (1), the spatial inhomogeneity drive is

$$\frac{\nabla F_0}{F_0} = \nabla\ln n + \left[\frac{m}{2T}(v_\perp^2 + (v_\parallel - u)^2) - \frac{3}{2}\right]\nabla\ln T - \frac{u}{v_\parallel}\frac{1}{T}\mu\nabla B + \frac{e}{T}\left(1 - \frac{u}{v_\parallel}\right)\nabla\Phi + \frac{m}{T}(v_\parallel - u)\nabla u.$$

For a high aspect ratio tokamak $B\sim 1/R$, so we can write

$$\nabla u = R\nabla\omega_\phi + \omega_\phi\nabla R = R\nabla\omega_\phi - u\frac{\nabla B}{B}$$

and thus,

$$\frac{\nabla F_0}{F_0} = \nabla\ln n + \left[\frac{m}{2T}(v_\perp^2 + (v_\parallel - u)^2) - \frac{3}{2}\right]\nabla\ln T + \frac{m}{T}(v_\parallel - u)R\nabla\omega_\phi - \frac{m}{T}u\left[(v_\parallel - u) + \frac{\mu B}{m}\frac{1}{v_\parallel}\right]\frac{\nabla B}{B} + \frac{e}{T}\left(1 - \frac{u}{v_\parallel}\right)\nabla\Phi. \tag{5}$$

The derivative with respect to energy is

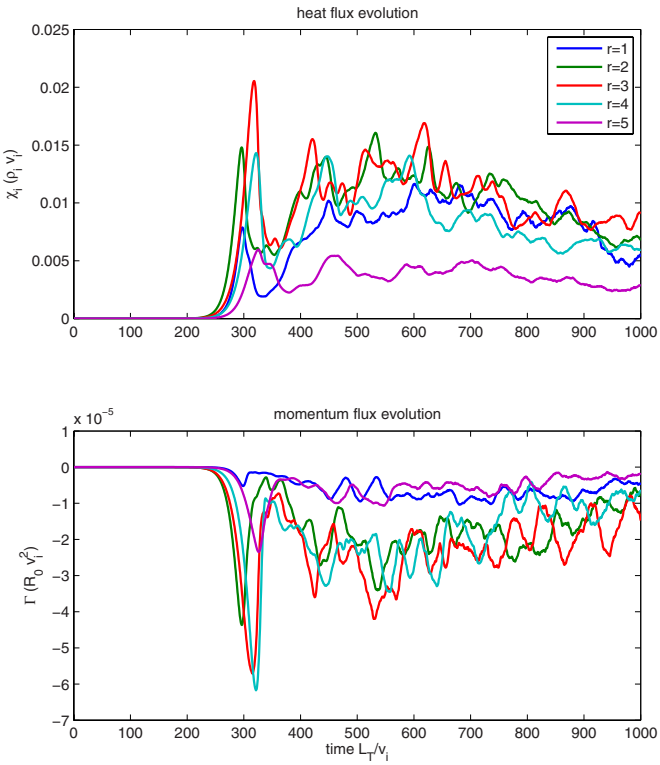

FIG. 1. (Color online) Ion heat conductivity (top panel) and toroidal momentum flux (bottom panel) evolution at different radial locations ($\omega_\phi=0.2v_i/R_0$).

$$\frac{1}{F_0}\frac{\partial F_0}{\partial\varepsilon} = -\frac{1}{T}\frac{1}{v_\parallel}(v_\parallel - u). \tag{6}$$

Substituting Eqs. (5) and (6) into Eq. (4), we get the gyrokinetic equation for the perturbed part of ion's distribution function

$$\frac{1}{F_0}\left[\frac{\partial}{\partial t} + (v_\parallel\hat{\mathbf{b}} + \mathbf{v}_E + \mathbf{v}_d)\cdot\nabla + e(v_\parallel\hat{\mathbf{b}} + \mathbf{v}_E + \mathbf{v}_d)\cdot\nabla\delta\phi\frac{\partial}{\partial\varepsilon}\right]\delta f = -\kappa\cdot\tilde{\mathbf{v}}_E - \frac{e}{T}(v_\parallel - u)\hat{\mathbf{b}}\cdot\nabla\delta\phi + \frac{1}{T}\left[\mu B + m(v_\parallel + u)(v_\parallel - u)\right]\frac{\nabla B}{B}\cdot\tilde{\mathbf{v}}_E, \tag{7}$$

where

$$\kappa \equiv \frac{\nabla n}{n} + \left[\frac{1}{T}\left(\mu B + \frac{m}{2}(v_\parallel - u)^2\right) - \frac{3}{2}\right]\frac{\nabla T}{T} + \frac{m}{T}(v_\parallel - u)R\nabla\omega_\phi$$

is the equilibrium density, temperature, and toroidal angular velocity gradients. The last term in κ would be vanishing in case of rigid rotation with ω_ϕ=const. The parallel nonlinearity term is not included in current simulations.

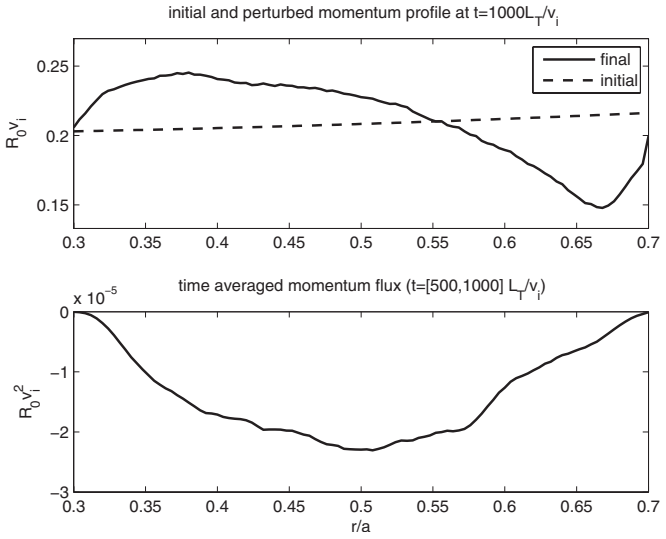

FIG. 2. Toroidal momentum and momentum flux profiles for $\omega_\phi = 0.2 v_i/R_0$.

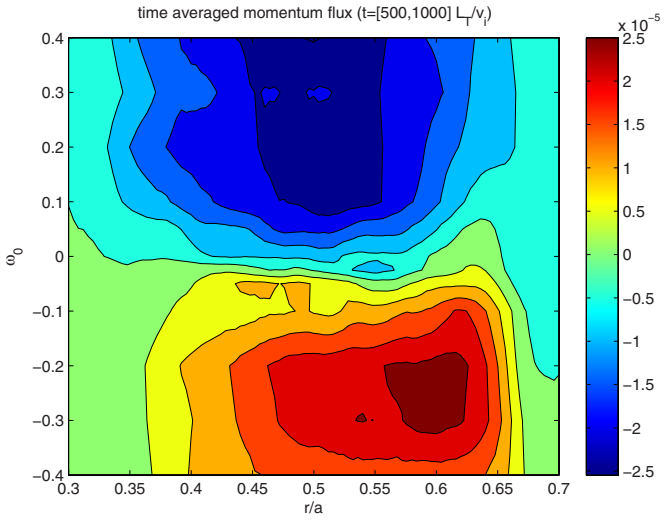

FIG. 4. (Color online) Off-diagonal part of the momentum flux (angular velocity ω_0 is normalized by v_i/R_0 and momentum flux is normalized by $R_0 v_i^2$).

III. RESULTS AND DISCUSSION

In our simulations, toroidal momentum transport is driven by ITG turbulence with the following parameters: $R_0/L_T=9$, $R_0/L_n=3$, $R_0/\rho_i=700$, $R_0/a=3$, and $T_e/T_i=1$, where R_0 and a are the tokamak major and minor radii, respectively; L_T and L_n are the equilibrium temperature and density inhomogeneity scale lengths, respectively; T_e and T_i are the electron and ion temperatures respectively; and ρ_i is the ion gyro radius.

As the result of simulations we produce the evolution of perturbed toroidal angular momentum $\langle \delta L_\phi \rangle \equiv \langle R v_\parallel \delta f \rangle$ and dominant[29] toroidal momentum flux $\Gamma_\phi \equiv \langle \delta L_\phi \delta v_r \rangle$. Here, δv_r is the radial component of the perturbed $E \times B$ drift velocity, and $\langle \cdots \rangle$ denotes the flux surface averaging.

We have started by considering the cases of rigid plasma rotation, i.e. setting constant mean angular velocity. The evolution of ITG turbulence is shown in the Fig. 1 (top panel), where we plot the ion heat conductivity versus time for different radial locations. The corresponding time evolution of toroidal momentum flux is plotted in Fig. 1 (bottom panel). The initial and resulting radial profile of toroidal momentum together with time averaged momentum flux is shown in Fig. 2. As we can see, the significant redistribution of momentum is observed at quasi-steady state after nonlinear saturation. This redistribution has a pinchlike character with the momentum flux directed towards the center of tokamak. Similar situation is observed for the case of rigid rotation in the opposite direction in Fig. 3, where we also see the spinning up of a plasma in the central region caused by the inverse flux of (negative) momentum, which leads to the conclusion that pinch-like momentum flux is independent of rotation direction. The result of parameter scan with different values of rotation velocity is shown in Fig. 4. As we can see, the momentum flux increases with rotation velocity, reaching saturation at $\omega_\phi \sim 0.25 v_i/R_0$. The flux maximum is slightly shifted towards larger r/a for the negative rotation case. The breaking of the symmetry in the sign of ω_0 may arise from the buildup of a net toroidal rotation in the case with no background rotation.

The diffusive flux was studied by simulating plasma with the sheared toroidal angular velocity, taken in the form $\omega_\phi = (\omega_0 + \omega_1 r/a) v_i/R_0$. The results of simulations for different values of rotation shear are summarized in Table I.

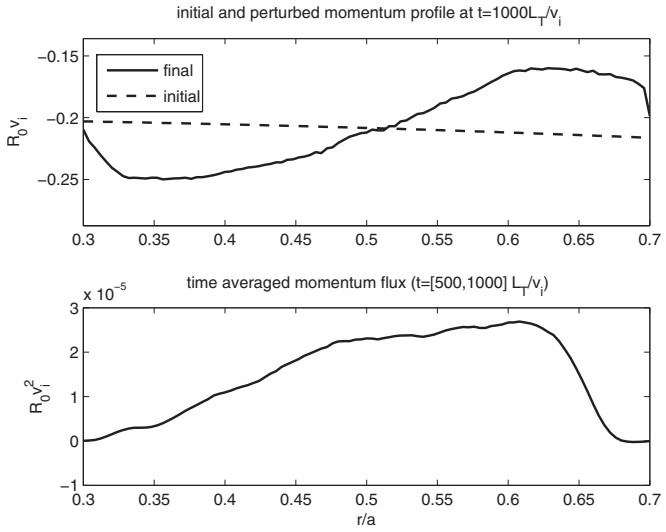

FIG. 3. Toroidal momentum and momentum flux profiles for $\omega_\phi = -0.2 v_i/R_0$.

TABLE I. Simulation results for sheared rotation cases.

ω_0	ω_1	$\Gamma_\phi(R_0 v_i^2)\times 10^{-5}$	$\chi_\phi^{\text{diff}}(\rho_i v_i)\times 10^{-3}$	$\chi_\phi^{\text{eff}}(\rho_i v_i)\times 10^{-3}$	$\chi_\phi^{\text{diff}}/\chi_i$
0.2	−0.4	0.52	4.1	2.9	0.41
0.15	−0.3	0.60	6.2	4.5	0.62
0.1	−0.2	0.32	6.4	3.6	0.6
−0.1	0.2	−0.37	2.3	4.2	0.23
−0.15	0.3	−0.63	3.6	4.7	0.36
−0.2	0.4	−0.58	2.4	3.3	0.24

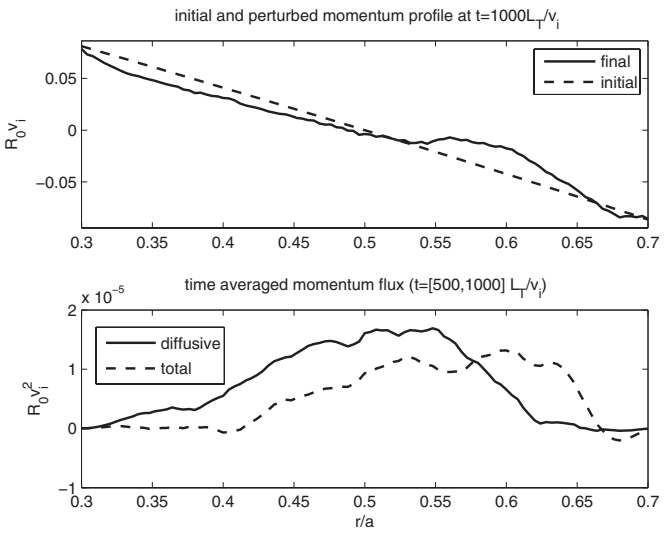

FIG. 5. Toroidal momentum and momentum flux profiles for $\omega_\phi=(0.2-0.4r/a)v_i/R_0$.

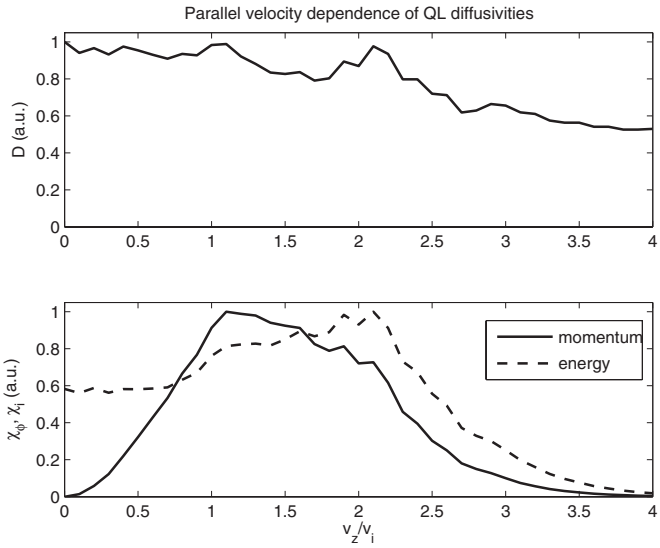

FIG. 6. Parallel velocity dependence of general (upper panel) and momentum and energy (lower panel) diffusivities based on quasilinear estimates.

The effective momentum conductivity is defined as $\chi_\phi^{\text{eff}} \equiv -\Gamma_\phi/\nabla L_\phi$, where Γ_ϕ is the total toroidal momentum flux, averaged in time and space. The diagonal part of momentum conductivity, i.e., the momentum diffusivity χ_ϕ^{diff}, is calculated by subtracting the off-diagonal (pinchlike) contribution from the total flux. This off-diagonal flux is calculated by interpolating data from the rigid rotation cases (Fig. 4). To illustrate the result of such subtraction, we plot in Fig. 5 the radial profiles of total and diffusive fluxes for the typical case with $\omega_0=0.2$ and $\omega_1=-0.4$. In this figure we clearly observe the redistribution of momentum resulting in profile flattening. The diffusive part of momentum flux turns out to be larger than the total flux in the region $r/a<0.5$, since diffusive and pinch fluxes have opposite directions in this region. The situation is inverse for $r/a>0.5$.

As we can see from Table I, the pinchlike and diagonal contributions can be comparable, especially in the low shear cases. The Prandtl number $\text{Pr}=\chi_\phi^{\text{diff}}/\chi_i$ is calculated based on the diagonal part of momentum conductivity. It is found to be in the range of $\text{Pr}\sim 0.2-0.7$, as shown in Table I.

Alternative calculations of momentum and heat conductivities can be done using quasilinear theory and fluctuation spectra obtained directly from simulations. Some discussions about validity and application of quasilinear theory for toroidal drift-wave turbulence can be found in Refs. 31–34. In particular, phase space islands overlapping is a necessary condition for stochastic diffusive process which should be satisfied.[32] Additional evidence of diffusiveness are the linear time dependence of the mean-square particle displacement $\langle \Delta r^2 \rangle$ and near-Gaussian probability density function for $\langle \Delta r \rangle$ (Refs. 33 and 35).

Following the transition probability formalism, the simple quasilinear expression for the mean-square radial displacement of the test particle's guiding center under the influence of the fluctuating electrostatic field can be derived,[34]

$$\frac{\langle \Delta x^2 \rangle}{\tau} = \frac{2\pi c^2}{B^2 V} \sum_{\mathbf{k}} \int_{-\infty}^{\infty} \frac{d\omega}{2\pi} \langle |\delta\phi^2| \rangle_{\omega,\mathbf{k}} k_y^2 J_0^2(k_\perp \rho_i)\, \delta(k_\parallel v_\parallel - \omega). \tag{8}$$

Here, $\langle |\delta\phi^2| \rangle_{\omega,\mathbf{k}}$ is the fluctuation spectral density, k_y is the poloidal wavevenumber, J_0 is the Bessel function of zeroth order, δ is the Dirac delta function, and V is the system's volume. The argument of δ-function represents parallel wave-particle resonance, the dominant decorrelation mechanism.[31]

Integrating the Fokker–Planck collision operator with corresponding weight, toroidal momentum and heat diffusivities can be found,

$$\chi_\phi^{QL} = \frac{1}{n\nabla(Rv_\parallel)} \int d\mathbf{v} R v_\parallel D(\mathbf{v})\, \nabla f(\mathbf{v}),$$
$$\chi_i^{QL} = \frac{1}{n\nabla T} \int d\mathbf{v} \frac{mv^2}{2} D(\mathbf{v})\, \nabla f(\mathbf{v}), \tag{9}$$

with the general radial diffusivity

$$D(\mathbf{v}) = \frac{1}{2}\frac{\langle \Delta x^2 \rangle}{\tau}. \tag{10}$$

The ratio of two diffusivities [Eq. (9)] is determined by the velocity dependence of general diffusivity $D(\mathbf{v})$, which itself is defined by the frequency dependence of fluctuation spectra in Eq. (8). The last one is found to be peaked at drift frequency $\omega \approx \omega_d(\varepsilon)$, corresponding to the energy $\varepsilon/T \approx 3$ and $v_\parallel/v_i \approx 2$.

We have found quasilinear diffusivity using fluctuation spectra obtained from simulations. After integration over perpendicular velocity, the parallel velocity dependence $D(v_\parallel)$ is shown in Fig. 6 (upper panel). It has a peak at $v_\parallel/v_i \approx 2$ which can be interpreted as the result of translation (by parallel wave-particle decorrelation[32]) of turbulence drive at $\omega = \omega_d$.

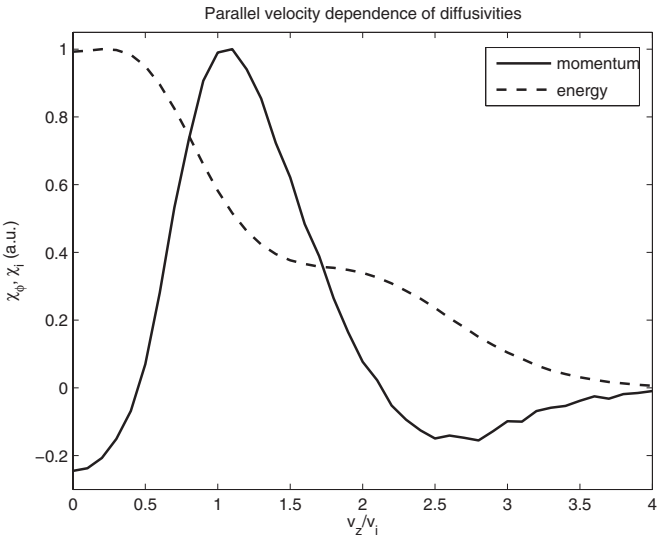

FIG. 7. Parallel velocity dependence of momentum and energy diffusivities obtained from simulations with $\omega_\phi=(0.2-0.4r/a)v_i/R_0$.

In typical tokamak experiments, the resonant energy is indeed larger than the thermal energy. Therefore, the thermal diffusivity χ_i^{QL} is larger than the momentum diffusivity χ_ϕ^{QL} for a shifted Maxwellian velocity distribution defined by Eq. (1) since χ_i^{QL} is weighted more than χ_ϕ^{QL} by higher particle energy. To confirm that, we plot the parallel velocity dependencies (Fig. 6, lower panel), which shows that quasilinear diffusivities are dominant at $v_\parallel/v_i>1$. The direct measurements from simulation also show similar picture (Fig. 7), although, there is negative nondiffusive contribution to momentum flux (discussed earlier in this section) which has not been captured by quasilinear estimates. The difference in heat conductivity dependence at small $v_\parallel$ can possibly be explained by use of simplified resonance condition in Eq. (8), which does not include perpendicular particle motion.

From the obtained quasilinear diffusivity (10), using expressions (8) and (9), we have found $\chi_\phi^{QL}/\chi_i^{QL}\approx 0.7$ in qualitative agreement with simulation results.

IV. SUMMARY

Global gyrokinetic simulations of toroidal momentum transport driven by ITG turbulence are performed, using the nonlinear gyrokinetic particle-in-cell code GTC. The equilibrium plasma rotation is described by a shifted Maxwellian parallel velocity distribution for ions. Cases with constant (rigid rotation) and radially sheared toroidal angular velocity are considered.

The temporal evolution together with the radial profiles of flux surface averaged toroidal momentum and momentum flux are obtained from the simulation. We observe a significant redistribution of toroidal momentum during the ITG instability development and after the nonlinear saturation. The general trend of spinning up of plasma towards the center of tokamak is observed for the rigid rotation cases, which is the manifestation of the off-diagonal (pinchlike) inward flux. For the sheared rotation cases, the competition between diffusive and off-diagonal fluxes takes place.

The obtained Prandtl number is found to be in the range from 0.2 to 0.7, which is in agreement with quasilinear estimate of $\mathrm{Pr}\sim 0.7$. It is smaller than unity since the resonant energy is usually larger than thermal energy.

In the future we are planning to study the effect of kinetic electrons by simulating momentum transport in a presence of trapped electron mode turbulence.

ACKNOWLEDGMENTS

The authors gratefully acknowledge useful discussions with P. H. Diamond, O. Gurcan, T. S. Hahm, and R. E. Waltz. The work was supported by DOE SciDAC GPS center under cooperative agreement DE-FC02-08ER54957. Simulations were performed using supercomputers at NERSC and ORNL.

[1] H. Biglari, P. H. Diamond, and P. W. Terry, Phys. Fluids B **2**, 1 (1990).
[2] T. S. Hahm and K. H. Burrell, Phys. Plasmas **2**, 1648 (1995).
[3] E. J. Strait, T. S. Taylor, A. D. Turnbull, J. R. Ferron, L. L. Lao, B. Rice, O. Sauter, S. J. Thompson, and D. Wroblewski, Phys. Rev. Lett. **74**, 2483 (1995).
[4] L. G. Eriksson, E. Righi, and K. D. Zastrow, Plasma Phys. Controlled Fusion **39**, 27 (1997).
[5] J. E. Rice, M. Greenwald, I. H. Hutchinson, E. S. Marmar, Y. Takase, S. M. Wolfe, and F. Bombarda, Nucl. Fusion **38**, 75 (1998).
[6] G. T. Hoang, P. Monier-Garbet, T. Aniel, C. Bourdelle, R. V. Budny, F. Clairet, L. G. Eriksson, X. Garbet, C. Grisolia, P. Platz, and J. C. Vallet, Nucl. Fusion **40**, 913 (2000).
[7] J. S. deGrassie, K. H. Burrell, L. R. Baylor, W. Houlberg, and J. Lohr, Phys. Plasmas **11**, 4323 (2004).
[8] L. Porte, S. Coda, S. Alberti, G. Arnoux, P. Blanchard, A. Bortolon, A. Fasoli, T. P. Goodman, Y. Klimanov, Y. Martin, M. Maslov, A. Scarabosio, and H. Weisen, Nucl. Fusion **47**, 952 (2007).
[9] B. P. Duval, A. Bortolon, A. Karpushov, R. A. Pitts, A. Pochelon, O. Sauter, A. Scarabosio, G. Turri, and the TCV Team, Phys. Plasmas **15**, 056113 (2008).
[10] Y. Sakamoto, S. Ide, M. Yoshida, Y. Koide, T. Fujita, H. Takenaga, and Y. Kamada, Plasma Phys. Controlled Fusion **48**, A63 (2006).
[11] J. E. Rice, A. Ince-Cushman, J. S. Degrassie, L. G. Eriksson, Y. Sakamoto, A. Scarabosio, A. Bortolon, K. H. Burrell, B. P. Duval, C. Fenzi-Bonizec, M. J. Greenwald, R. J. Groebner, G. T. Hoang, Y. Koide, E. S. Marmar, A. Pochelon, and Y. Podpaly, Nucl. Fusion **47**, 1618 (2007).
[12] K. Ida, T. Minami, Y. Yoshimura, A. Fujisawa, C. Suzuki, S. Okamura, S. Nishimura, M. Isobe, H. Iguchi, K. Itoh, S. Kado, Y. Liang, I. Nomura, M. Osakabe, C. Takahashi, K. Tanaka, and K. Matsuoka, Phys. Rev. Lett. **86**, 3040 (2001).
[13] N. Mattor and P. H. Diamond, Phys. Fluids **31**, 1180 (1988).
[14] A. G. Peeters and C. Angioni, Phys. Plasmas **12**, 072515 (2005).
[15] J. S. deGrassie, D. R. Baker, K. H. Burrell, P. Gohil, C. M. Greenfield, R. J. Groebner, and D. M. Thomas, Nucl. Fusion **43**, 142 (2003).
[16] K. D. Zastrow, W. G. F. Core, L. G. Eriksson, M. G. Von Hellermann, A. C. Howman, and R. W. T. Konig, Nucl. Fusion **38**, 257 (1998).
[17] S. D. Scott, P. H. Diamond, R. J. Fonck, R. J. Goldston, R. B. Howell, K. P. Jaehnig, G. Schilling, E. J. Synakowski, M. C. Zarnstorff, C. E. Bush, E. Fredrickson, K. W. Hill, A. C. Janos, D. K. Mansfield, D. K. Owens, H. Park, G. Pautasso, A. T. Ramsey, J. Schivell, G. D. Tait, W. M. Tang, and G. Taylor, Phys. Rev. Lett. **64**, 531 (1990).
[18] P. C. de Vries, K. M. Rantamaki, C. Giroud, E. Asp, G. Corrigan, A. Eriksson, M. d. Greef, I. Jenkins, H. C. M. Knoops, P. Mantica, H. Nordman, P. Strand, T. Tala, J. Weiland, K. D. Zastrow, and JET EFDA Contributors, Plasma Phys. Controlled Fusion **48**, 1693 (2006).
[19] P. H. Diamond, V. B. Lebedev, Y. M. Liang, A. V. Gruzinov, I. Gruzinova, M. Medvedev, B. A. Carreras, D. E. Newman, L. Charlton, K. L. Sidikaman, D. B. Batchelor, E. F. Jaeger, C. Y. Wang, G. G. Craddock, N. Mattor, T. S. Hahm, M. Ono, B. LeBlanc, H. Biglari, F. Y. Gang, and D. J. Sigmar, in *Proceedings of the 15th IAEA Fusion Energy Conference*, Seville, 1994 (IAEA, Vienna, 1996), IAEA-CN-60/D-13, Vol. 3, p. 323.

[20]L. Chen, J. Geophys. Res., [Space Phys.] **104**, 2421, DOI: 10.1029/1998JA900051 (1999).
[21]A. G. Peeters, C. Angioni, and D. Strintzi, Phys. Rev. Lett. **98**, 265003 (2007).
[22]O. D. Gurcan, P. H. Diamond, T. S. Hahm, and R. Singh, Phys. Plasmas **14**, 042306 (2007).
[23]T. S. Hahm, P. H. Diamond, O. D. Gurcan, and G. Rewoldt, Phys. Plasmas **14**, 072302 (2007).
[24]T. S. Hahm, P. H. Diamond, O. D. Gurcan, and G. Rewoldt, Phys. Plasmas **15**, 055902 (2008).
[25]P. H. Diamond, C. J. McDevitt, O. D. Gurcan, T. S. Hahm, and V. Naulin, Phys. Plasmas **15**, 012303 (2008).
[26]O. D. Gurcan, P. H. Diamond, and T. S. Hahm, Phys. Rev. Lett. **100**, 135001 (2008).
[27]A. Eriksson, H. Nordman, P. Strand, J. Weiland, T. Tala, E. Asp, G. Corrigan, C. Giroud, M. de Greef, I. Jenkins, H. C. M. Knoops, P. Mantica, K. M. Rantamaki, P. C. de Vries, and K. D. Zastrow, Plasma Phys. Controlled Fusion **49**, 1931 (2007).
[28]J. E. Kinsey, G. M. Staebler, and R. E. Waltz, Phys. Plasmas **12**, 052503 (2005).
[29]R. E. Waltz, G. M. Staebler, J. Candy, and F. L. Hinton, Phys. Plasmas **14**, 122507 (2007).
[30]Z. Lin, T. S. Hahm, W. W. Lee, W. M. Tang, and R. B. White, Science **281**, 1835 (1998).
[31]I. Holod and Z. Lin, Phys. Plasmas **14**, 032306 (2007).
[32]Z. Lin, I. Holod, L. Chen, P. H. Diamond, T. S. Hahm, and S. Ethier, Phys. Rev. Lett. **99**, 265003 (2007).
[33]W. L. Zhang, Z. Lin, and L. Chen, Phys. Rev. Lett. **101**, 095001 (2008).
[34]S. Ichimaru, *Basic Principles of Plasma Physics. A Statistical Approach* (Benjamin, New York, 1973), p. 256.
[35]Z. Lin, S. Ethier, T. S. Hahm, and W. M. Tang, Phys. Rev. Lett. **88**, 195004 (2002).